N79-22623

NASA Technical Memorandum 79137

PRELIMINARY COMPARISON OF THEORY AND EXPERIMENT FOR A CONICAL, PRESSURIZED-FLUIDIZED-BED COAL COMBUSTOR

(NASA-TM-79137) PRELIMINARY COMPARISON OF THEORY AND EXPERIMENT FOR A CONICAL, PRESSURIZED-FLUIDIZED-BED COAL COMBUSTOR (NASA) 56 p HC A04/MF A01 CSCL 10A G3/44

N79-22623

Unclas 23983

R. W. Patch
Lewis Research Center
Cleveland, Ohio

March 1979

PRELIMINARY COMPARISON OF THEORY AND EXPERIMENT FOR A CONICAL, PRESSURIZED-FLUIDIZED-BED COAL COMBUSTOR

by R. W. Patch
NASA Lewis Research Center
Cleveland, OH 44135

SUMMARY

A published model and ancillary computer programs were used for a comparison of theory with an actual conical, pressurized-fluidized-bed combustor burning caking bituminous coal and using limestone to reduce sulfur dioxide emission. It was necessary to make a number of changes to the source programs to get meaningful results. In addition, the inputs of limestone density, adjustable elutriation parameter, and heat transfer coefficient were adjusted to compensate for limitations in the model. Theoretical bed pressure drop was in good agreement with experiment. The burnable carbon elutriated indicated that, contrary to the assumption in the theory, the exhaust port was below the transport disengaging height, resulting in disagreement between theory and experiment. The observed nitrogen oxides emission rate was about half the theoretical value. There was order-of-magnitude agreement on sulfur dioxide emission rates. Recommendations for improving the model are given.

INTRODUCTION

The pressurized-fluidized-bed coal combustor is being investigated by the Department of Energy, the utility industry, and several laboratories with the ultimate purpose of achieving clean coal combustion in high-efficiency central-station powerplants (refs. 1, 2, and 3). In such systems, the ability to scale up small combustors

to larger sizes is of great importance. Ideally, the best way to scale up such combustors would be with a realistic physical model as opposed to multiple regression correlations or empirical scaling laws. The primary purpose of this report is to give preliminary comparisons between a physical model (ref. 4) and a conical pressurized-fluidized-bed combustor (refs. 5 and 6) and attempt to explain any discrepancies. A secondary purpose of this report is to provide additional information for anyone using the two complementary computer programs published in reference 4. The scope of this work did not include a systematic check of the equations used in the model nor the computer programs. A number of discrepancies are reported which were discovered in the course of attempting to run the programs. Most of these were corrected.

Previous work modeling fluidized bed combustors has been somewhat limited. Horio and Wen (ref. 7) used a modified bubble assemblage model with distributions of coal particle size and limestone conversion to calculate sulfur dioxide removal efficiency by limestone additive. Horio and Wen (ref. 8) later published a treatment of elutriation of fines, solids mixing, combustion efficiency, and bed temperature profile. Chen and Saxena (ref. 9) included both sulfur dioxide removal efficiency and combustion efficiency and were first with a three-phase comprehensive model. Concurrent work in modeling includes that of the MIT Energy Laboratory staff (ref. 10) and that of Rajan, Krishnan, and Wen (ref. 11).

All the previous modeling work mentioned applies to fluidized bed combustors of constant cross-sectional area. This report is the first comparison of a variable cross-sectional area (conical) fluidized bed combustor with a model (ref. 4). The conical bed has the advantage that it minimizes elutriation (ref. 5). The realism of the model was improved by using the actual bed particle density, which was measured three ways.

APPARATUS

Conical, Pressurized, Fluidized Bed Combustor

The pressurized fluidized bed combustor and associated systems are shown in a simplified schematic in figure 1. Geometrically, the combustor consisted of a lower 24.7 inch high cylindrical section of 8.8 inch inside diameter, a middle 7.3 inch high truncated-cone section of 10.48° cone half angle, and an upper 79.9 inch high truncated cone section of 3.40° cone half angle, bringing the inside diameter at the top to 21 inches. There were six ports spaced vertically on the side of the combustor. A solids removal auger could be located in any one of the ports to maintain the level of the bed inside the combustor no higher than that port.

A mixture of coal and limestone was injected into the bottom of the combustor using high pressure air as a transport media. The fuel (coal plus limestone) flow was controlled by the rotational speed of the fuel metering screw, which was calibrated in terms of flow. Pressurized air at ambient temperature flowed into the bottom of the reactor through a distributor containing a total of 36 holes 1/8 inch in diameter in nine bubble caps.

Heat was removed from the bed via banks of water-cooled horizontal heat-exchanger tubes. Three banks of seven tubes per bank were installed in the bottom two feet of the bed.

The limestone-to-coal ratio was determined from the rotation rates of the coal and limestone metering screws, which were calibrated for flow rates. The air feed rate was determined with venturi meters. Other details are given in reference 5.

Cylindrical Cold-Flow Atmospheric Fluidized Bed

A cylindrical fluidized bed was used to measure the minimum fluidization velocity and void fraction of bed material taken from the conical combustor. This was part of one method of determining particle density of spent bed material. The apparatus is shown in figure 2. The fluidizing gas was dry air. The inlet temperature of the air was measured with an alcohol-in-glass thermometer in an oil-filled thermometer well. Flow was manually controlled with a throttle valve and read on a rotometer. The reading was corrected for pressure variations by means of a bourdon-tube pressure gage upstream. The bed was contained in a transparent plastic column with a fine wire mesh distributor near the bottom. The top of the bed was at ambient pressure. Bed pressure drop was measured with a diaphragm pressure gage.

MODEL

The theoretical model for the conical, pressurized fluidized bed coal combustor is given in reference 4 (the "Level II" model), but will be reviewed briefly here.

Hydrodynamics

It is assumed that "fast" bubbles are present (rising velocity of bubble greater than gas velocity in emulsion). Hence, the bubbles have clouds. The bubble size is given by the correlation of Mori and Wen (ref. 12) modified for a combustor of varying cross-sectional area. Char mixing is calculated from a single-phase back-flow multicell model. Limestone is assumed to be completely mixed. Gas flow is based on a two-phase theory, where the emulsion is one phase and the bubbles and clouds are the other phase. A gas interchange coefficient between the two phases is included.

Coal Combustion

A spherical particle model is employed for coal combustion. Only the lean case is treated. The hydrogen and oxygen volatize immediately upon injection of coal into the combustor, not changing the diameter of the resultant char. The diameter is gradually reduced by burning with oxygen, with the rate determined by the surface rate of chemical reaction and gas diffusion. Ash particles break off as the char burns. Carbon, nitrogen, and sulfur in the char are assumed to be released or used at the same rate as the char burns.

Limestone Chemical Kinetics

A porous constant diameter sphere model is employed for limestone chemical kinetics. The limestone is assumed to calcine as soon as it is injected into the combustor, producing pores. The reaction rate with sulfur dioxide is given by Borgwardt's (ref. 13) model.

Nitrogen Oxides Kinetics

Nitrogen oxides are assumed to be produced only from coal-bound nitrogen. A numerical fit to the experimental results of Ruth (ref. 14) was made, assuming the quantity of nitrogen oxides produced is directly proportional to the BTU's of the coal actually burned and nonlinearly proportional to the excess air.

Heat Balance

A multicell single-phase backmix model is employed. The overall heat transfer coefficient to the heat exchanger tubes must be given. The heat transferred to the walls and radiated from the top of the bed is assumed to be zero.

Elutriation

Elutriation of char, ash, and limestone are treated differently. For char it is assumed that the combustor exhaust gas port is above the transport disengaging height, and one of three empirical correlations may be selected for the elutriation rate. The fraction of ash elutriated is not calculated so it must be given as an input. The limestone is assumed not to elutriate.

COMPUTER PROGRAMS

General Description

The detailed model (Level II) is too complex even for a high-speed digital computer. Hence a simplified model is used to estimate the loss of burnable carbon due to elutriation and the combustion efficiency. The program for this simplified model is called Level I.

Level I Program

This program assumes plug flow or back mixing of gas (plug flow was assumed in this report). It assumes complete mixing of solids and an isothermal cylindrical bed. The coal fed is assumed to have a size distribution. The bed temperature must be given. The size distribution of the char is solved for, taking into account combustion, elutriation, and solids withdrawal. This requires three nested iteration loops. The inner loop is for B_{cf} (symbols are given in Appendix A), which is related to the ratio of coal particles fed to char particles withdrawn. The middle loop is for Θ, which is the mean residence time of limestone. The outer loop is for η_c, which is the combustion efficiency. Outputs include the loss of burnable carbon due to elutriation.

Level II Program

This program assumes a bed of any geometry, size distribution of coal, and size distribution of limestone. Inputs include η_c and the loss of burnable carbon due to elutriation, both from Level I. It solves the rest of the equations described in the MODEL section of this report, including bed temperature and burnable carbon concentration as functions of height.

Changes to Programs

A few changes to the two programs were made merely for convenience, such as changes to output format. However, other changes were programmed that affected the outputs. These are given below, where all card numbers refer to the numbers on the left on pages 62-91 of reference 4.

Level I Program

Changes are given in Table I. Here MAIN refers to the main Level I program. These changes were not 100 percent successful. In 45 cases, B_{cf} did not converge 348 times, but always converged on the final iteration. This is believed related to the change in subroutine POP to eliminate incorrect negative values of ϕ. The differential equation for ϕ is solved from y = 0 to y = 1. If it were solved from y = 1 to y = 0, it is believed negative values of ϕ would never occur even without the change in POP in Table I. Also, in two cases the exponential in POP was out of range. Attempts to correct this were abandoned.

Level II Program

Changes are given in Table II. These changes appear to have been successful.

PROGRAM TEST CASES AND ADJUSTMENT OF CONSTANTS

Test Cases

Level I Program

A test case is given in reference 4, but the input contains some errors: SCF should read XCF, DPF(7) should be 0.1003 instead of 0.1, and EXAIR should be 0.06 instead of 0.13. With these changes (but not the changes in Table I), the outputs from an IBM-360 computer at NASA checked reference 4 (see Table III) although the residence time Θ did not converge. With the changes in Table I, the outputs were different (see Table III), although the only outputs used as inputs in Level II (ETC (combustion efficiency) and ELOSS (carbon elutriated)) were not much different.

Level II Program

A test case is given in reference 4, but the input contains some errors: ATB(1) and ATB(2) should be 4180.6 instead of 4181.0, ZB(4) should be 150. instead of 200.0, ZHE(4) should be 300. instead of 200.0, ZDIS(1) should be 66. instead of 0.0, DNZL should be .37338 instead of 0.3734, DEAV should read DZAV, and EXAIR should be .174 instead of 17.4. With these changes (but not the changes in Table II) the outputs in reference 4 were obtained. With the changes in Table II, the output was as given in Table IV. The only large change is in ANOX(NO_x).

Preliminary Results and Comparisons

For comparison, five experimental steady-state tests with a total duration of 20 hours and 7 minutes were run under the same conditions with the discharge solids removal auger in port #3 (see figure 1). Caking bituminous coal from the Pittsburgh #8 seam was used with Grove City, Virginia limestone. The material loaded in the bed prior to the tests was bed material from previous tests using the same kind of coal and limestone. The results of the tests were averaged and are given in Tables V and VI as well as figure 3, figure 4, and Appendix B. The methods of calculating or obtaining inputs for Level I and Level II programs are given in Appendix B for the quantities which were not changed in later calculations for the five averaged tests.

The input quantities which were changed later were HLMF (bed height), DPL (limestone diameter), BETA (adjustable elutriation parameter), DB (bubble diameter), and RHOLS (limestone density) in Level I; and ELLOSS (carbon elutriated), RHOAD (limestone density), ETCA (estimated combustion efficiency), NDPAD (number of limestone sizes), DPADF (limestone size), FRACTA (fraction of limestone of a size), and UHEAV (heat transfer coefficient) in Level II. We shall call the preliminary cases for the five averaged tests Case 1a, Case 1b, and Case 1c for elutriation correlations from references 15, 16, and 17, respectively (corresponding to IELUTR of 1, 2, and 3 in Level I). For Cases 1a, 1b, and 1c, the above input quantities were calculated or obtained as given in Appendix C.

Outputs from Level I and II programs are given in Tables V and VI, respectively, along with observed values (observed ELOSS (carbon elutriated) was obtained using a fly ash burnable carbon fraction determined by measuring carbon on a sample previously washed with dilute phosphoric acid to eliminate all carbonates). The calculated fraction of burnable carbon elutriated (ELOSS) was far lower than observed for all three elutriation correlations (refs. 15-17). However, Case 1a (IELUTR = 1 so reference 15 used for elutriation) was closest (see figure 3).

For Case 1a, the bed temperature was too high, sulfur retention was too low, fractional conversion of additive was too low, and sulfur dioxide and nitrogen oxides in the exhaust were too high compared to observed values. In addition, there was slight agreement between

calculated and observed size distribution of elutriated carbon (see figure 4), the observed carbon being much smaller than the predicted carbon.

Changes to Input Data and Comparisons

Case 2a

The particle density of a bed of porous particles such as limestone in various degrees of calcination and sulfation is difficult to measure because it is supposed to be based on the actual mass of the particles and a volume that includes both the solids and the pores but not the interstices. Different fluids used in measuring the particle density go into the pores to various degrees. To find a realistic particle density for the spent bed of the conical fluidized bed combustor, the measurement on the spent bed was made in three ways: (1) a pyknometer with Jet A kerosene gave a density of 2.73 g/cm^3; (2) a mercury porosimeter gave densities of 2.29 and 3.05 g/cm^3 at pressures of 1.8 and 15000 psia, respectively; (3) a cylindrical cold flow fluidized bed (figure 2) gave a minimum fluidization velocity which in conjunction with a dry sieving analysis gave a particle density of 2.62 g/cm^3. The last of the three results (2.62) was then compared with the particle densities calculated for the bed (calcined limestone) in Level I and II programs. The calculated particle densities were too low. Consequently, the fictitious limestone densities needed to give a bed particle density of 2.62 g/cm^3 were calculated and were 4.89 and 4.57 g/cm^3 for Level I and II, respectively (see Table V and VI). In Level I, the spend bed dry sieving analysis and equation (C1) gave a

DPL (limestone size) of 0.0793 cm. From equations (C7) - (C11), DB (bubble diameter) was 13.75 cm. From equations (C12) - (C13) HLMF (bed depth) was 62.4 cm. In Level II DPADF (limestone size), NDPAD (number of limestone sizes), and FRACTA (fraction in limestone size) were taken from the dry sieving analysis of the spent bed (columns 1 and 4 of Table VII). The resulting Level I and II outputs are given in Tables V and VI, respectively. ETS (sulfur capture), FS (limestone conversion), and XGO(3) (SO_2 in offgas) were much closer to the observed values, while ELOSS (carbon elutriated), ETC (combustion efficiency), and T (temperature) were slightly worse.

Case 3a

To get Level I to reproduce the observed ELOSS (carbon elutriated), BETA (elutriation parameter) was adjusted to 25. The Level I and II outputs are given in Tables V and VI, respectively.

Case 4a

To get T (temperature) at 36 cm above the top of the distributor to agree with the observed value, UHEAV (heat transfer coefficient) was adjusted to 1.083×10^{-2} cal/cm^2 sec K. This compensated for the lack of wall heat transfer and radiant heat transfer from the top of the bed in Level II. The Level I and II outputs are given in Tables V and VI, respectively.

The constants for Case 4a were used for Cases 5 to 30 below, but in Level I the variables WCOAL (coal flow), CABS (calcium to sulfur ratio), EXAIR (excess air), P (pressure), TK (temperature), DT (bed diameter), HLMF (bed depth), DB (bubble diameter), and PASH (ash

elutriated) were changed to conform to the results of the new experiments described below. In Level II, ELLOSS (carbon elutriated), ETCA (estimated combustion efficiency), HLF (bed height), PAV (bed pressure), TAV (temperature), WCOAL (coal flow), CABS (calcium to sulfur ratio), PF (pressure below distributor), EXAIR (excess air), and GZCO (ratio of CO to C in coal) were also changed to conform.

END RESULTS AND DISCUSSION

Twenty-six new tests of about four hours each were run at different conditions but with coal and limestone from the same source. The calcium-to-sulfur ratio, excess air, bed pressure, bed depth, and bed temperature were varied. Level I and II programs were used to predict observable quantities for the 26 tests (Cases 5 to 30). The results are given in figures 5-12.

Figure 5 gives observed and calculated bed pressure drop. The agreement tends to justify the use of the fictitious limestone densities. The wild point is probably due to an instrumentation problem.

Figure 6 gives observed and calculated fraction of burnable carbon elutriated. The scatter is great. The four most likely reasons for the scatter are: (1) the exhaust port is below the transport disengaging height so it gets splashed by particles from bursting bubbles. This is confirmed by figure 13; (2) char attrition was neglected; (3) Size segregation with height due to hydrodynamic effects was neglected (this is very pronounced for spent bed material in the cylindrical bed, figure 2); and (4) char thermal decrepitation was neglected.

Figure 7 gives observed and calculated combustion inefficiency. Most of the combustion inefficiency is due to solid carbon elutriated or discharged. The observed values are based on bomb calorimeter data for both fly ash and discharge. The scatter is partly due to all the observed burnable carbon fractions in the discharge being measured as zero or less due to basic problems with using a bomb calorimeter for this application (negative carbon fractions were arbitrarily set equal to zero).

Figure 8 gives observed and calculated nitrogen oxides emission rate. The calculated values tend to be too high. Ruth (ref. 14) states that "Larger combustors can be expected to emit even less NO_x because of more uniform temperatures and lower combustion intensities." Since Ruth had a 4.5 inch i.d. combustor compared to our 8.8 inch i.d. combustor, this is consistent with figure 8. In addition, Beer et al. (ref. 18) have pointed out that nitric oxide is partially reduced by reaction with char in the bed. This reduction would be more pronounced in our combustor than Ruth's because on the average our bed was deeper and, due to the conical shape, had a lower superficial velocity near the top.

Figure 9 shows observed and calculated bed temperature. The reason for the scatter is not known, but may be due to difficulties in measuring the fuel feed rate by means of the fuel metering screw.

Figures 10, 11, and 12 give observed and calculated sulfur emission rate, efficiency of sulfur capture, and calcium utilization, respectively. These are all related. The agreement with theory was very limited. Multiple regression analyses did better, showing moderate scatter for sulfur emission rate and efficiency of sulfur capture about the regression equations, but large scatter for calcium utilization. The extremes of sulfur emission rate are so wide that one or both of two mechanisms are suspected: (1) raw coal is transported by bubbles to the top surface of the bed once in a while, or (2) hot spots are formed in the bed, causing the limestone to lose SO_2 there (ref. 19). The scatter in calcium utilization is probably due to the duration of each test being considerably shorter than the residence time of the limestone (24 to 174 hours) so the condition of the limestone is influenced by previous tests.

In many cases the bed temperature from the Level II program increased with height all the way from the 36 cm level to the top of the bed. The increase was as much as 8.8%. Experimentally the increase never exceeded 0.5%, and generally the temperature decreased with height or was essentially constant. The difficulty is there is no wall heat transfer in the Level II model (and radiant heat transfer from the top of the bed was neglected but may be important).

Some of the lack of agreement between Level II output and observed values may be due to the impossibility of making a valid adjustment to the wake-to-bubble volume ratio f_w in the program due to insufficient experimental data. The quantity f_w determines the degree of solids mixing and could be adjusted if burnable carbon as a function of height were measured, or wall heat transfer was included in the program.

Another contributor to lack of agreement between Level I and II output and observed values may be the bubble sizes assumed in the programs, which, as the authors point out (ref. 4), have never been verified for conical beds with heat transfer tubes in the bed. It appeared that the calculated bubble sizes were larger than observed with closed-circuit television (fig. 1).

In general, the results from Level I and II were not as good as multiple regression analyses in correlating the experimental data, although one would hesitate to trust a multiple regression analysis for gross extrapolations.

CONCLUSIONS AND RECOMMENDATIONS

1. Bed pressure drop from theory and experiment were in good agreement.
2. Measured burnable carbon elutriated was 21 times the theoretical value until the value of an adjustable parameter was changed from 1 to 25.
3. The observed average size of char elutriated was about one-third the theoretical value.

4. The observed nitrogen oxides emission rate was about half the theoretical value.

5. There was order-of-magnitude agreement between theory and experiment on sulfur dioxide emission rate.

6. The published digital computer program is not fully operational, and the computer results were inferior to multiple regression analysis for correlating the data.

7. The theoretical burnable carbon elutriated should be improved by including a correlation for exhaust port below the transport disengaging height and perhaps one or more of the following: (1) char attrition, (2) char thermal decrepitation, or (3) char segregation by hydrodynamic forces.

8. The bubble size correlation should be verified for conical beds with heat exchanger tubes in the bed.

9. The theory should include wall heat transfer (and perhaps radiant heat transfer from the top of the bed).

10. The theoretical mixing should be adjusted by means of an empirical factor, preferably by measurement of burnable carbon as a function of height in the bed.

APPENDIX A - SYMBOLS

Mathematical	Level I FORTRAN	Level II FORTRAN	
A_t			Area of top of bed
	ALAMA		Average value of y^2 (number basis)
	ALAMV		Average value of y^3 (number basis)
		AHE	Specific heat transfer area of heat exchanger tubes
		ANOX	Mole fraction NO_x in the effluent gas
		ATB	Cross sectional area of combustor at specified heights
B_{cf}	BC1		Coal feed rate (number basis) multiplied by B_{cw} and divided by char withdrawal rate (number basis)
B_{cw}	BC		Dimensionless ratio (see ref. 4)
	BETA		Adjustable parameter for elutriation calculations
		BEDVOL	Total bed volume
c			Wet coal feed rate divided by air feed rate
	CABS	CABS	Mole ratio of calcium to sulfur in the feed solids
		CADF	Heat capacity of limestone fed
		CCF	Heat capacity of coal fed
		CELU	Elutriation rate of solid carbon

Mathematical	Level I FORTRAN	Level II FORTRAN	
		CGMF	Molar heat capacity of feed gas at feed temperature
		CLOSS	Total carbon loss to solids
D_B	DB		Average bubble diameter
D_{BM}			Maximum bubble diameter
D_{BO}			Initial bubble diameter
d_ℓ	DPL		Mean diameter of limestone particles
$d_{\ell,i}$			Mean diameter of limestone particles in size interval i
	DPF	DPCF	Diameter of coal fed to combustor at various sieve sizes
	DT		Bed diameter
		DNZL	Diameter of distributor holes
		DPADF	Diameter of limestone fed to combustor at various sieve sizes
		DTHICK	Distributor plate thickness
		DTUBE	Outside diameter of heat exchanger tubes
		DZAV	Specified compartment height for calculations
E	EXAIR	EXAIR	Excess air ratio
	EC		Quantity used in elutriation calculations (see ref. 4)
	ELOSS	ELLOSS	Fraction of burnable carbon elutriated
	EMF		Void fraction of bed at minimum fluidization

Mathematical	Level I FORTRAN	Level II FORTRAN	
		ETS	Efficiency of sulfur capture
F_m	FMO		Total molar flow rate of gas in the bed
f_w		FW	Volume ratio of wake to bubble
	FRACT(I)	FRACTC(I)	Weight fraction of coal fed to combustor between DPF(I-1) and DPF(I)
		FD	Fraction of solids discharged from bed at each discharge location (excluding elutriated solids)
		FFAD	Fraction of limestone fed at each solids feed location
		FFC	Fraction of coal fed at each solids feed location
		FRACTA(I)	Weight fraction of limestone fed to combustor between DPADF(I-1) and DPADF(I).
		FS	Fractional conversion of limestone
g			Acceleration of gravity
		GZCO	Ratio of moles of CO formed to moles of C in coal fed
		GZH2	Ratio of moles of H_2 formed to sum of moles of H_2 formed, moles of H_2O formed, and moles of moisture in coal fed
		GZH2S	Ratio of moles of H_2S formed to total moles of S in feed
	HCHAR		Hold-up of char in bed
	HRC		Mass fraction of carbon in bed

Mathematical	Level I FORTRAN	Level II FORTRAN	
		HAREA	Total heat transfer area
		HLF	Height of the fluidized (expanded) bed
	IELUTR		Selector for elutriation correlation (1 for ref. 15, 2 for ref. 16, or 3 for ref. 17)
	IMODEL		Selector for gas flow model (2 for plug flow)
		IARR	Selector for arrangement of heat exchanger tubes (0 for none, 3 for horizontal inline)
		IGNITE	Selector for cold flow or combustor (1 for combustion)
L_{mf}	HLMF	HLMF	Minimum fluidization bed height
M_{air}			Molecular weight of air
M_C, M_{Ca}, M_{H2}, M_{H2O}, M_{N2}, M_{O2}, M_S			Molecular weight of species indicated
		MDIS	Number of solids discharge locations
		MFEED	Number of solids feed locations
		MTB	Number of heights where ATB is given
		MTHE	Number of heat exchanger sections, including sections with none
n_d		AND	Number of distributor holes
	N	NDPC	Number of members of FRACT or FRACTC array

Mathematical	Level I FORTRAN	Level II FORTRAN	
		NDPAD	Number of members of FRACTA array
p	P	PAV	Average absolute pressure in bed
	PASH		Fraction of ash elutriated
		PF	Absolute gas pressure below the distributor
		PH	Horizontal pitch of heat exchanger tubes
		PV	Vertical pitch of heat exchanger tubes
		QAREA	Heat transfer rate to heat exchangers per unit area
		QCOAL	Lower heating value of wet coal
		QTRANS	Total heat transferred to heat exchangers
		QVOL	Heat transfer rate to heat exchangers per unit volume of bed
R			Universal gas constant
	RHOC		True density of coal
		SOLVOL	Apparent volume of solids in bed
$\bar{T}$	TK	TAV	Average bed temperature (initial estimate in case of Level II)
		T	Bed temperature
		TETUBE	Total volume fraction of heat exchanger tubes

Mathematical	Level I FORTRAN	Level II FORTRAN	
		TF	Inlet gas temperature
		TWAV	Average heat exchanger coolant temperature
u_{mf}			Superficial gas velocity at minimum fluidization
u_o	UO		Superficial gas velocity in bed at $\bar{T}$ and p
		UHEAV	Average overall heat transfer coefficient between bed and heat exchanger coolant
		UF	Superficial gas velocity at the distributor at TF and PF
V_{cone}			Volume of fluidized conical bed
	VCF		Volumetric flow of coal feed excluding voids
	VCW		Volumetric withdrawal rate of solids excluding voids
	VLS		Volumetric feed rate of limestone excluding voids
	VMF	VMF	Volume of bed at minimum fluidization everywhere (hypothetical for conical bed)
w_c	WCOAL		Dry coal feed rate by weight
	WBED		Total bed weight
		WAD	Total limestone feed rate by weight
		WCOAL	Wet coal feed rate by weight
		WDIS	Total discharge rate by weight

Mathematical	Level I FORTRAN	Level II FORTRAN	
		WELT	Solids elutriation rate by weight
X_i			Weight fraction in size interval i
x_C			Weight fraction total carbon in dry coal
x_H	XH	XH	Weight fraction hydrogen in dry coal
$x_{\ell,Ca}$	XLCA		Weight fraction calcium in limestone
x_m	XW	XW	Weight fraction moisture in coal (dry basis)
x_N	XN	XN	Weight fraction nitrogen in dry coal
x_O	XO	XO	Weight fraction oxygen in dry coal
x_S	XS	XS	Weight fraction sulfur in dry coal
	XCF	XCF	Weight fraction fixed carbon in dry coal
	XCV	XCV	Weight fraction volatile carbon in dry coal
	XGO		Mole fraction oxygen in effluent gas
		XAV	Average burnable carbon concentration in the bed, weight basis
		XCACO3	Weight fraction $CaCO_3$ in limestone
		XGF	Feed gas composition
		XGO(1)	Mole fraction O_2 in effluent gas

Mathematical	Level I FORTRAN	Level II FORTRAN	
		XGO(2)	Mole fraction CO_2 in effluent gas
		XGO(3)	Mole fraction SO_2 in effluent gas
		XGO(4)	Mole fraction H_2O in effluent gas
		XMGCO3	Weight fraction $MgCO_3$ in limestone
y			Ratio of char diameter to maximum char diameter
$y_{O2,0}$	XGOO		Mole fraction O_2 in the feed gas
Z_{cyl}			Bed depth of equivalent cylindrical bed
		ZB	Height above distributor where ATB specified
		ZDIS	Height of solids discharge above distributor
		ZF	Height of solids feed above distributor
		ZHE	Height of tops of heat exchanger sections (including sections with no heat exchangers)
ε_B			Volume fraction of bubbles
η_c	ETC	ETC	Combustion efficiency
		ETCA	Initial estimate of combustion efficiency
Θ	THET		Mean residence time of limestone

Mathematical	Level I FORTRAN	Level II FORTRAN	
μ			Viscosity of gas in bed
ρ_g			Density of gas in bed
$\rho_{\ell s}$	RHOLS	RHOAD	True density of limestone
ρ_s			Bed particle density
ϕ			Distribution function for char in bed, number basis

Note: "Wet" coal means coal as received from producer.

APPENDIX B - METHODS OF CALCULATING OR OBTAINING INPUTS TO PROGRAMS FOR CASES 1a, 1b, 1c, 2a, 3a, AND 4a

This appendix gives methods of calculating or obtaining inputs to Level I and II for the five averaged tests for those inputs which were the same for Cases 1a, 1b, 1c, 2a, 3a, and 4a. Values are also given.

Level I Inputs

XCF

This was obtained from the proximate analysis of coal and was 0.5340.

XCV

This was obtained from the proximate and ultimate analyses of coal and was 0.2198.

XH, XS, XO, and XN

These were obtained from the ultimate analysis of coal and were 0.0514, 0.0199, 0.0761, and 0.0149, respectively.

XW

This was obtained from the proximate analysis of coal and was 0.0217.

N, DPF, and FRACT

These were obtained by dry sieving coal taken from between the metering screw and the blending auger. N was 19, and DPF as well as FRACT are given in Table VII.

WCOAL

This was obtained from the rotation rate of the fuel metering screw and the limestone-to-coal ratio and was 4.51 g/sec.

CABS

The limestone-to-coal ratio was obtained from rotation rates of the limestone and coal metering screws. Then CABS was calculated from the limestone-to-coal ratio and chemical analyses of the limestone and coal and was 1.617.

EXAIR

This was obtained from the equation (ref. 4)

$$E = \frac{y_{O2,O}}{M_{air}(1 - X_m)c\left(\frac{X_c}{M_c} + \frac{X_H}{2M_{H2}} + \frac{X_S}{M_S} - \frac{X_O}{M_{O2}}\right)} - 1 \qquad (B1)$$

and had the value 0.639.

VO

This was 0 since EXAIR was specified.

P and TK

These were observed directly and had values of 5.15 atm and 1151K, respectively.

DT

This was taken from a drawing and was 36.4 cm.

PASH

This was measured with help from chemical analysis of fly ash and discharge solids and was 0.780.

IMODEL

This was 2 for plug flow of gas.

EMF

This was measured on spent bed material from the combustor in the cylindrical bed (fig. 2) and was 0.51.

RHOC

This was measured on the coal in a pyknometer with Jet A kerosene and was 1.267 g/cm^3.

XLCA

This was obtained from chemical analysis of the limestone and was 0.383.

Level II Inputs

In addition to the quantities already given for Level I, some of which are also used in Level II:

CADF

From reference 20 the specific heat of limestone is 0.217 cal/g C.

CCF

From references 21 and 22 using the Kirov approximation, the specific heat of the wet (as received) coal is 0.3139 cal/g K.

CGMF

From references 23 and 24, the specific heat of air is 6.955 cal/mole K.

MTB, ZB, and ATB

From drawings MTB is 4, ZB(1) - ZB(4) are 0., 62.7, 81.3, and 280. cm; and ATB(1) - ATB(4) are 405., 405., 670., and 2193 cm^2.

MTHE, ZHE, AHE, DTUBE, PV, PH, and IARR

MTHE was 5. See Table VIII for values of other variables from drawings.

MFEED, ZF(1), FFC(1), and FFAD(1)

From drawings the values were 1, 6.91 cm, 1., and 1., respectively.

MDIS, ZDIS(1), and FD(1)

From drawings the values were 1, 141.94 cm, and 1., respectively.

AND, DNZL, and DTHICK

The values were 36., 0.317 cm, and 1.27 cm, respectively.

DZAV

To be consistent with Table VIII, a value of 8 cm was used.

FW

The value of 0.15 in the test case (ref. 4) was used.

XCACO3 and XMGCO3

Values were obtained from chemical analysis of the limestone and were 0.9575 and 0.0107.

QCOAL

The higher heating value was measured in an ASTM bomb calorimeter and converted to a lower heating value of 7109 cal/g.

NDPC, DPCF, and FRACTC

NDPC was 19. DPCF and FRACTC are given in Table VII.

HLF, VMF, and HLMF

HLF from drawings was 141.94 cm (only one of these three quantities need be given; the others are then set to 0).

PAV and TAV

Same as P and TK in Level I.

TWAV

Measured as 298K.

WCOAL

Calculated the same as in Level I except for wet (as received) basis, so value was 4.62 g/sec.

WAD and CABS

CABS was same as in Level I (only one of these two quantities need be given; the other is then 0).

UF

This is always set to 0 if EXAIR is specified.

TF and PF

Measured as 297K and 5.47 atm, respectively.

XGF

For air (ref. 24) the values of XGF(1)-XGF(7) were 0.21, 0., 0., 0., 0., 0., and 0., respectively.

GZCO and GZH2

These were measured as 4.45×10^{-4} and 0., respectively.

GZH2S

Since all cases were lean, this was assumed to be 0.

IGNITE

Assuming combustion, the value was 1.

APPENDIX C - METHODS OF CALCULATING OR OBTAINING INPUTS TO PROGRAMS FOR CASES 1a, 1b, AND 1c

This appendix gives methods of calculating or obtaining inputs to Level I and II for the five averaged tests for those inputs which were not the same for Cases 1a, 1b, 1c, 2a, 3a, and 4a and applies to Cases 1a, 1b, and 1c only. Values are also given.

Level I Inputs

DPL

The limestone was dry sieved (see Table VII). The mean diameter (DPL) was then found from (ref. 4)

$$d_\ell = \frac{1}{\sum_i \frac{X_i}{d_{\ell,i}}} \tag{C1}$$

and was 0.0790 cm.

RHOLS

The true density of the limestone was measured in a pyknometer with Jet A kerosene and was 2.66 g/cm^3.

DB

First F_m was found from the equation (ref. 4).

$$F_m = w_c \left\{ \frac{(1+E)X_c}{M_c y_{O2,O}} \left[\left(\frac{X_H}{2M_{H2}} + \frac{X_S}{M_S} - \frac{X_O}{M_{O2}} \right) \frac{M_c}{X_c} + 1 \right] + \frac{X_H}{2M_{H2}} + \frac{X_O}{M_{O2}} + \frac{X_N}{M_{N2}} + \frac{X_{MI}}{M_{H2O}} \right\} \tag{C2}$$

Next u_0 was found from

$$u_o = \frac{F_m R \bar{T}}{\rho A_t} \tag{C3}$$

Viscosity was found from (ref. 4)

$$\mu = 3.72 \times 10^{-6} \bar{T}^{0.676} \tag{C4}$$

Gas density was found from

$$\rho_g = \frac{\rho M_{air}}{R \bar{T}} \tag{C5}$$

Bed particle density was found from (ref. 4 with change from Table I)

$$\rho_s = \rho_{ls} X_{l,Ca} \frac{56.08}{M_{Ca}} \tag{C6}$$

Minimum fluidization velocity was found from (ref. 4)

$$u_{mf} = \frac{\mu}{d_l \rho_g} \left\{ \left[33.7^2 + .0408 \frac{d_l^3 \rho_g (\rho_s - \rho_g) g}{\mu^2} \right]^{1/2} - 33.7 \right\} \tag{C7}$$

Maximum bubble diameter was found from (ref. 4)

$$D_{Bm} = 0.652 \left[A_t (u_o - u_{mf}) \right]^{0.4} \tag{C8}$$

Initial bubble diameter was found from (ref. 4)

$$D_{BO} = 0.347 \left[\frac{A_t (u_o - u_{mf})}{n_d} \right]^{0.4} \tag{C9}$$

The bed depth for the equivalent cylindrical bed was found from

$$Z_{cyl} = \frac{V_{cone}}{A_t} \tag{C10}$$

Finally D_B was found from (ref. 4)

$$D_B = D_{Bm} - (D_{Bm} - D_{Bo})\, e^{-\frac{0.15\, Z_{cyl}}{D_t}} \tag{C11}$$

and was 16.00 cm.

HLMF

First the bubble fraction was found from (ref. 4)

$$\varepsilon_B = \frac{1}{1 + \frac{0.711\sqrt{g\, D_B}}{u_o - u_{mf}}} \tag{C12}$$

Then the minimum fluidization bed height (HLMF) was found from (ref. 4)

$$L_{mf} = \frac{V_{cone}\,(1 - \varepsilon_B)}{A_t} \tag{C13}$$

and was 57.5 cm.

BETA

This is a parameter to adjust to match the experiment. It was taken to be one because this would be its value if the elutriation correlations were directly applicable.

Level II Inputs

RHOAD

Same as RHOLS in Level I inputs.

NDPAD, DPADF, and FRACTA

NDPAD was 19. DPADF and FRACTA are given in columns 1 and 3 of Table VII.

UHEAV

Measured as 7.65×10^{-3} cal/sec cm^2 K.

REFERENCES

1. Energy Conversion Alternatives Study (ECAS) Summary Report. NASA TM-73871, 1977.

2. Anson, D.: Fluidized Bed Combustion of Coal for Power Generation. Prog. Energy Combust. Sci., vol. 2, no. 2, 1976, pp. 61-82.

3. Rao, Charagundla S. R.: Fluidized-Bed Combustion Technology - A Review. Combust. Sci. Technol., vol. 16, no. 6, 1977, pp. 215-227.

4. Horio, M.; Rengarajan, P.; Krishnan, R.; and Wen, C. Y.: Fluidized Bed Combustor Modeling (West Virginia University; NASA Contract NAS3-19725.) NASA CR-135164, 1977.

5. Priem, R. J.; Rollbuhler, R. J.; and Patch, R. W.: Effluent Characterization from a Conical Pressurized Fluid Bed. NASA TM-73897, 1977.

6. Zellars, Glenn R.; Rowe, Anne P.; and Lowell, Carl E.: Erosion/Corrosion of Turbine Airfoil Materials in the High-Velocity Effluent of a Pressurized Fluidized Coal Combustor. NASA TP-1274, 1978.

7. Horio, M.; and Wen, C. Y.: Analysis of Fluidized Bed Combustion of Coal with Limestone Injection. Fluidization Technology. Vol. II. Dale L. Keairns, ed., Hemisphere Publ. Corp., 1976, pp. 289-320.

8. Horio, M.; and Wen, C. Y.: Simulation of Fluidized Bed Combustors: Part 1. Combustion Efficiency and Temperature Profile. Am. Inst. Chem. Eng. Symp. Series, vol. 74, no. 176, 1978, pp. 101-111.

9. Chen, Tan-Ping; and Saxena, Satish C.: Mathematical Modelling of Coal Combustion in Fluidized Beds with Sulfur Emission Control by Limestone or Dolomite. Fuel, vol. 56, no. 4, Oct. 1977, pp. 401-413.

10. Louis, J. F.; Tung, S. E.; and Williams, G. C., eds.: Modeling of Fluidized Bed Combustion of Coal Final Reports - Executive Summary. HCP/T2295-01, Energy Research and Development Admin., 1978.

11. Rajan, R.; Krishnan, R.; and Wen, C. Y.: Simulation of Fluidized Bed Combustors: Part II. Coal Devolatilization and Sulfur Oxides Retention. Am. Inst. Chem. Eng. Symp. Series, vol. 74, no. 176, 1978, pp. 112-119.

12. Mori, S.; and Wen, C. Y.: Estimation of Bubble Diameter in Gaseous Fluidized Beds. Am. Inst. Chem. Eng. J., vol. 21, no. 1, Jan. 1975, pp. 109-115.

13. Borgwardt, Robert H.: Kinetics of the Reaction of SO_2 with Calcined Limestone. Environ. Sci. Technol., vol. 4, no. 1, Jan. 1970, pp. 59-63.

14. Ruth, Lawrence A.: Combustion and Desulfurization of Coal in a Fluidized Bed of Limestone. Fluidization Technology. Vol. II. Dale L. Keairns, ed., Hemisphere Publ. Corp., 1976, pp. 321-327.

15. Zenz, F. A. and Weil, N. A.: A Theoretical Empirical Approach to the Mechanism of Particle Entrainment from Fluidized Beds. Am. Inst. Chem. Eng. J., vol. 4, no. 4, 1958, pp. 472-479.

16. Kunii, Daizo and Levenspiel, Octave: Fluidization Engineering. John Wiley and Sons, Inc., 1969, pp. 313-317. (Primary Source - Yagi, S.; and Aoji, T.: Elutriation of Fines from a Fluidized Bed. Paper presented at the Soc. of Chem. Engrs. (Japan), Fall Meeting, 1955 (in Japanese).)

17. Wen, Chin-Yung and Hashinger, Richard F.: Elutriation of Solid Particles from a Dense-Phase Fluidized Bed. Am. Inst. Chem. Eng. J., vol. 6, no. 2, 1960, pp. 220-226.

18. Beer, Janos M.; Sarofim, Adel F.; Chan, Lisa K.; and Sprouse, Alice M.: NO Reduction by Char in Fluidized Combustion. Proceedings of the Fifth International Conference on Fluidized Bed Combustion, M78-68, Vol. II, The Mitre Corp., 1978, pp. 577-592.

19. Glenn, R. D. and Robison, E. B.: Characterization of Emissions from Fluidized-Bed Combustion of Coal and Control of Sulfur Emission with Limestone. Proceedings of Second International Conference on Fluidized-Bed Combustion. U.S. Environmental Protection Agency, AP-109, 1972, pp. II-2-1 to II-2-8.

20. Perry, Robert H. and Chilton, Cecil H.: Chemical Engineer's Handbook. Fifth ed. McGraw-Hill Book Co., Inc., 1973, pp. 3-136.

21. Preparation of a Coal Conversion Systems Technical Data Book. FE-1730-21, Energy Research and Development Admin., 1976.

22. Keenan, Joseph H. and Keyes, Frederick, G.: Thermodynamic Properties of Steam, Including Data for the Liquid and Solid Phases. John Wiley and Sons, Inc., 1936.

23. JANAF Thermochemical Tables. Dow Chemical Company, 1960, Rev. through 1978.

24. U.S. Standard Atmosphere, 1976. NOAA-s/T 76-1562, NASA TM X-74335, 1976.

TABLE I. - CHANGES TO LEVEL I PROGRAM

Program or subprogram	Purpose	Change
ALL	Obtain sufficient numerical accuracy so θ will converge	Run on UNIVAC 1100 series computer instead of IBM 360 (both in single precision).
MAIN	Obtain consistent value of density of calcined limestone	Change card 22 from RHOL = RHOLCA to RHOL = RHOLCA * 56.08 / MCA
MAIN	Eliminate use of D for two different quantites at same time	Change card 57 from D = 4.26 * (TK / 1800.) ** 1.75 / P to DO2 = 4.26 * (TK / 1800.) ** 1.75 / P
MAIN	Put particle diameters in increasing order to facilitate numerical integration	Delete card 128. Change card 130 from IF(K.EQ.N) GO TO 21 to 16 IF(K.EQ.N) GO TO 21 Insert after card 132 IF(XX.GT.DPF(K)) GO TO 19 DP(L) = XX Insert after card 133 GO TO 17 19 DP(L) = DPF(K) PHIF(L) = FRACT(K) GO TO 16
MAIN	Eliminate use of D for two different quantities at same time	Insert after card 142 D = DO2
MAIN	Obtain correct mass feed rate of uncalcined limestone	Change card 201 from WLS = CABS * WCOAL * XS * MCA / MS to WLS = CABS * WCOAL * XS * MCA / (MS * XLCA)
MAIN	Obtain correct volumetric feed rate of limestone	Change card 202 from VLS = WLS / RHOLCA to VLS = WLS / RHOLS
MAIN	Obtain θ convergence	Change card 211 from DTH = -THETM * 0.25 to DTH = -THETM * 0.1
MAIN	Obtain θ convergence	Change card 225 from THET = THETM / (1. + TH1 * ETC) to THET = THETM
MAIN	Obtain B_{cf} convergence	Change card 243 from DBC1 = 100. to DBC1 = 10. Change card 244 from DO 50 IBC1 = 1, 20 to DO 50 IBC1 = 1, 200
MAIN	Eliminate use of A1 for two different quantities at same time	Change card 288 from A1 = AT / (WBED * EC) to AAAA = AT / (WBED * EC) Change card 301 from YC1 = DP(I) ** 3 * A1 * AKE(I) * PHI(I) to YC1 = DP(I) ** 3 * AAAA * AKE(I) * PHI(I)
POP	Eliminate negative values of ϕ	Insert after card 29 IF(PHI(I).LT.0.) PHI(I) = 0.

TABLE II. - CHANGES TO LEVEL II PROGRAM

Program or subprogram	Purpose	Change
Main	Make NO_x correlation agree with reference 14	Change card 468 from ANOX = AN * WCOAL * (1. - ETC) * QCOAL / FMO to ANOX = AN * WCOAL * ETC * QCOAL / FMO
HYDRO	Obtain correct values of bed volume	Insert after card 843 BEDVOL = BEDVOL - DVBB(I)
VOLUME	Get HLMF, VMF, and HLF to be consistent no matter which is nonzero on input	Change card 954 from A = 1.0 - (ZZ - Z(N)) / DZAV to A = - (ZZ - Z(N)) / DZAV

TABLE III. - OUTPUT FOR LEVEL I TEST CASE

Quantity (see appendix A)	Value from reference 4 or IBM 360 computer at NASA	Value with changes in table I using UNIVAC 1100 series computer
ETC	0.9291	0.9327
XGO	0.5332×10^{-7}	0.3316
THET, sec	0.1859×10^{5}	0.1793×10^{5}
BC	0.1005	0.1070
BC1	0.1701×10^{3}	0.1650×10^{3}
VCW, cm^3/sec	0.8210×10^{-1}	0.1889
VCF, cm^3/sec	0.2086×10^{2}	0.2086×10^{2}
VLS, cm^3/sec	0.2309×10^{1}	0.2309×10^{1}
HCHAR, g	0.1386×10^{4}	0.3077×10^{4}
WBED, g	0.7832×10^{5}	0.9296×10^{5}
HRC	0.1375×10^{-1}	0.2571×10^{-1}
EC, 1/sec	0.1131×10^{-6}	0.1065×10^{-6}
ELOSS	0.6694×10^{-1}	0.5821×10^{-1}
ALAMV	0.1236×10^{-3}	0.2971×10^{-3}
ALAMA	0.7792×10^{-3}	0.1081×10^{-2}

TABLE IV. - OUTPUT FOR LEVEL II TEST CASE

Quantity (see appendix A)	Value from reference 4	Value with changes in table II using UNIVAC 1100 series computer
ETC	0.9282	0.9282
XAV	0.1547×10^{-1}	0.1547×10^{-1}
TAV, K	0.7759×10^{3}	0.7757×10^{3}
ETS	0.8287	0.8288
FS	0.3767	0.3767
XGO(1)	0.4560×10^{-1}	0.4560×10^{-1}
XGO(2)	0.1635	0.1635
XGO(3)	0.3500×10^{-3}	0.3498×10^{-3}
XGO(4)	0.5742×10^{-1}	0.5742×10^{-1}
ANOX	0.1839×10^{-4}	0.2377×10^{-3}
HLF, cm	0.6705600×10^{2}	0.6706×10^{2}
HLMF, cm	0.4842171×10^{2}	0.4843×10^{2}
VMF, cm^3	0.1791724×10^{6}	0.1792×10^{6}
BEDVOL, cm^3	0.3013810×10^{6}	0.3014×10^{6}
SOLVOL, cm^3	0.1791724×10^{6}	0.1792×10^{6}
TETUBE	0.1131662	0.1132
HAREA, cm^2	0.2526380×10^{5}	0.2526×10^{5}
QTRANS, cal/sec	0.7488019×10^{5}	0.7485×10^{5}
QVOL, cal/sec cm^3	0.2484568	0.2484
QAREA, cal/sec cm^2	0.2963932×10^{1}	0.2963×10^{1}
WELT, g/sec	0.2945155×10^{1}	0.2945×10^{1}
CELU, g/sec	0.7362888	0.7363
CLOSS, g/sec	0.7550509	0.7551
WDIS, g/sec	0.1215159×10^{1}	0.1215×10^{1}

TABLE V. - IMPORTANT INPUT AND OUTPUT FOR LEVEL I PROGRAM FOR PRELIMINARY RESULTS (CASE 1a, 1b & 1c) AND CHANGES (CASES 2a, 3a & 4a).

OBSERVED VALUES FOR THE FIVE AVERAGED TESTS ARE GIVEN FOR COMPARISON

Case	Inputs						Outputs			
	Minimum fluidization bed height, HLMF cm	Mean diameter of limestone, DPL cm	Adjustable parameter for elutriation, BETA	Average bubble diameter, DB cm	Limestone true density, RHOLS g/cm^3	Selector for elutriation correlation, IELUTR	Combustion efficiency, ETC	Limestone residence time, THET sec	B_{CW} x coal feed rate ÷ char withdrawal rate, BC1	Fraction of burnable carbon elutriated, ELOSS
1a	57.5	0.0790	1.	16.00	2.66	[a]1	0.999108	1.231×10^5	13.43	8.08×10^{-4}
1b	57.5	.0790	1.	16.00	2.66	[b]2	.999846	1.231×10^5	12.77	6.15×10^{-5}
1c	57.5	.0790	1.	16.00	2.66	[c]3	.999885	1.231×10^5	12.50	1.57×10^{-5}
2a	62.4	.0793	1.	13.75	4.89	[a]1	.999455	2.03×10^5	13.10	4.91×10^{-4}
3a&4a	62.4	.0793	25.	13.75	4.89	[a]1	.990778	2.04×10^5	17.36	1.048×10^{-2}
Observed		.0790			2.66		.9895			1.048×10^{-2}

[a]Elutriation per reference 15.

[b]Elutriation per reference 16.

[c]Elutriation per reference 17.

TABLE VI. - IMPORTANT INPUT AND OUTPUT FOR LEVEL II PROGRAM FOR PRELIMINARY RESULTS (CASE 1a) AND CHANGES (CASES 2a, 3a & 4a).

OBSERVED VALUES FOR THE FIVE AVERAGED TESTS ARE GIVEN FOR COMPARISON.

Case	Inputs			Outputs					
	Limestone true density, RHOAD g/cm^3	Size distribution of limestone, NDPAD, DPADF, FRACTA for	Overall heat transfer coefficient, UHEAV cal/cm^2 sec K	Combustion efficiency, ETC	Bed temperature, T[a] C	Efficiency of sulfur capture, ETS	Fractional conversion of limestone, FS	Mole fraction SO_2 in effluent, XGO(3)	Mole fraction NO_x in effluent, ANOX
1a	2.66	limestone	7.65×10^{-3}	0.9990	980	0.611	0.378	0.000408	0.000290
2a	4.57	spent bed	7.65×10^{-3}	0.9994	1005	.785	.485	.000225	.000290
3a	4.57	spent bed	7.65×10^{-3}	0.9876	1019	.834	.515	.000175	.000287
4a	4.57	spent bed	1.083×10^{-2}	.9876	878	.861	.532	.000146	.000287
Observed	2.66	limestone	7.65×10^{-3}	.9895	878	.792	.490	.000226	.000125

[a]Temperature at 36 cm above top of distributor.

TABLE VII. - RESULTS OF DRY SIEVING COAL, LIMESTONE, AND SPENT BED MATERIAL. QUANTITIES ARE INPUTS TO LEVEL I AND II PROGRAMS

Diameter at top of size interval, DPF, DPADF, or DPCF for all cases, cm	Weight fraction coal in size interval, FRACT or FRACTC for all cases	Weight fraction limestone in size interval, FRACTA[a] for cases 1a, 1b & 1c	Weight fraction spent bed in size interval, FRACTA[b] for cases 2a, 3a, 4a & 5-30
0.0074	0.0003	0.0123	
.0104	.0009	.0068	
.0147	.0069	.0135	
.0175	.0025	.0026	
.0208	.0163	.0032	
.0295	.0356	.0088	
.0351	.0425	.0053	0.0170
.0417	.0538	.0091	.0239
.0495	.0553	.0114	.0508
.0589	.0594	.0123	.0645
.0701	.0825	.0255	.1515
.0833	.0766	.0622	.1645
.0991	.1172	.1424	.1998
.1168	.0963	.1259	.1246
.1397	.0960	.1406	.0938
.1651	.1500	.1856	.0827
.1981	.0747	.1433	.0213
.2362	.0194	.0854	.0049
.2794	.0138	.0038	.0007

[a]For limestone from between limestone metering screw and blending auger.

[b]For spend bed material.

TABLE VIII. - SPECIFICATIONS OF HEAT EXCHANGER TUBES FOR LEVEL II

PROGRAM INPUT FOR ALL CASES

Height of top of section, ZHE cm	Specific heat transfer area, AHE 1/cm	Outside diameter of tube, DTUBE cm	Vertical pitch of tubes, PV cm	Horizontal pitch of tubes, PH cm	Selector for arrange-ment of tubes, IARR
24.	0.	0.	0.	0.	0.
40.	.1744	1.27	8.	2.86	3
48.	0.	0.	0.	0.	0.
56.	.1744	1.27	8.	2.86	3
280.	0.	0	0.	0.	0.

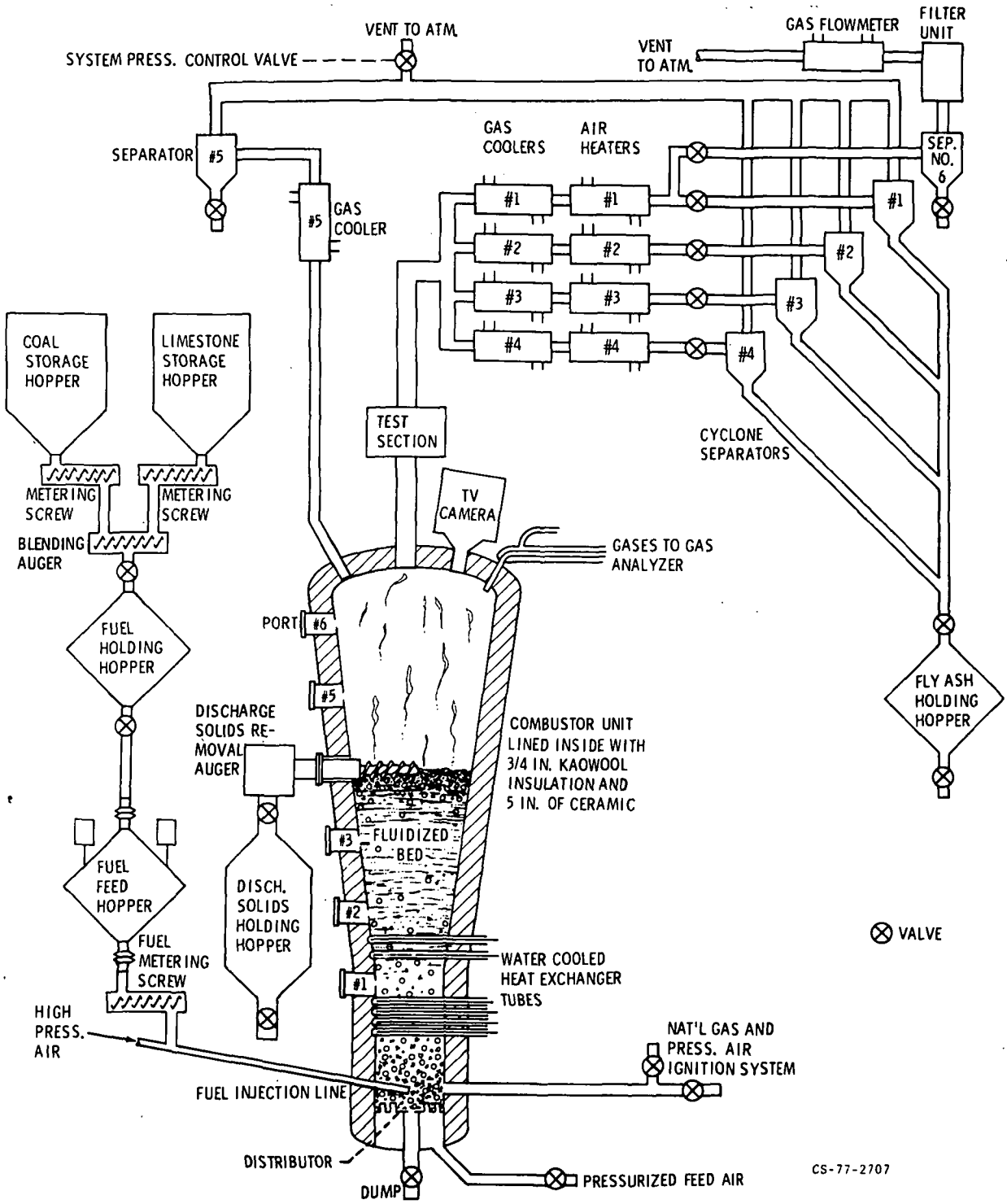

Figure 1. - Schematic of LeRC pressurized fluidized bed combustor.

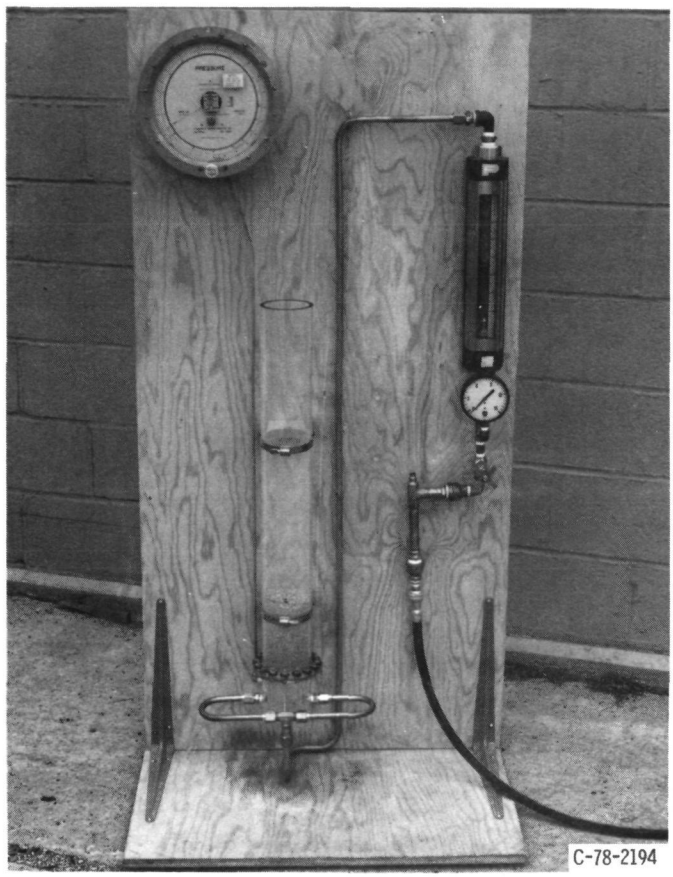

Figure 2. - Cylindrical cold-flow atmospheric fluidized bed used to measure particle density.

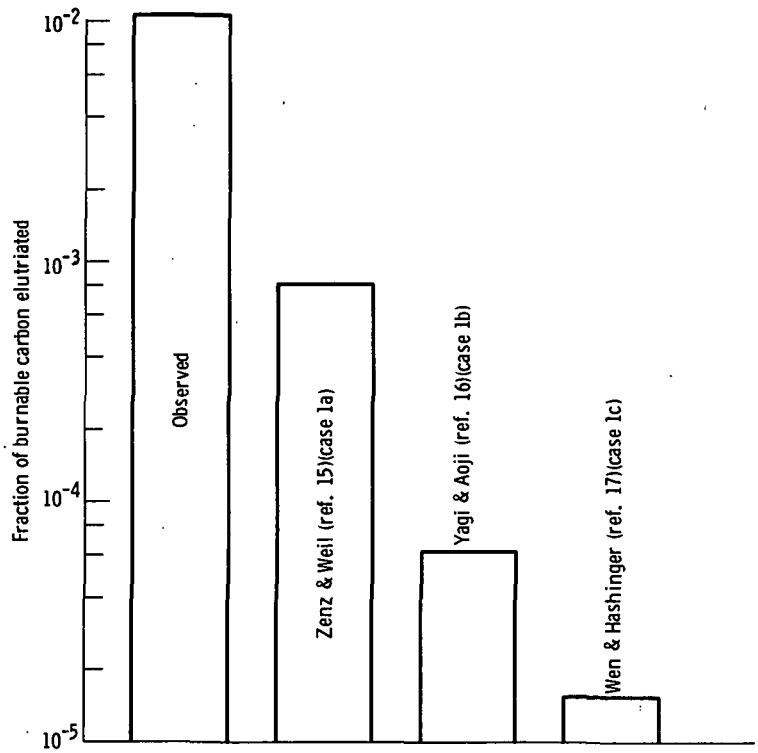

Figure 3. - Comparison of burnable carbon elutriated based on experiment and three elutriation correlations for preliminary results (BETA = 1).

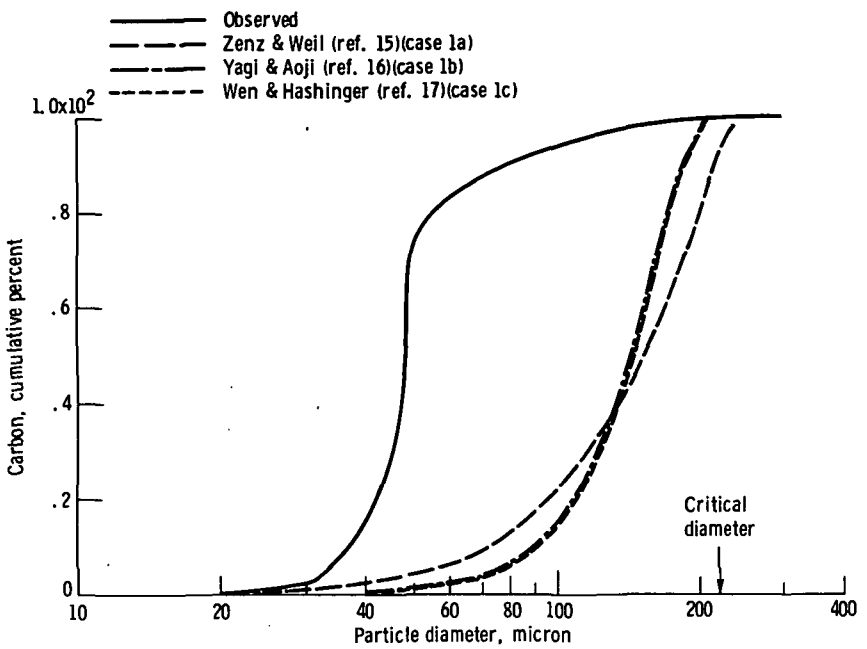

Figure 4. - Comparison of calculated and observed size distribution of elutriated carbon for preliminary results.

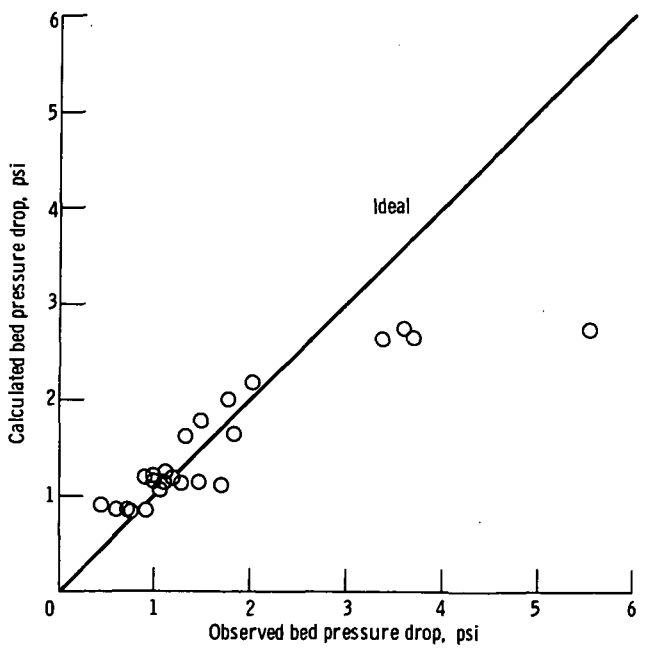

Figure 5. - Comparison of observed and calculated bed pressure drop for cases 5 to 30.

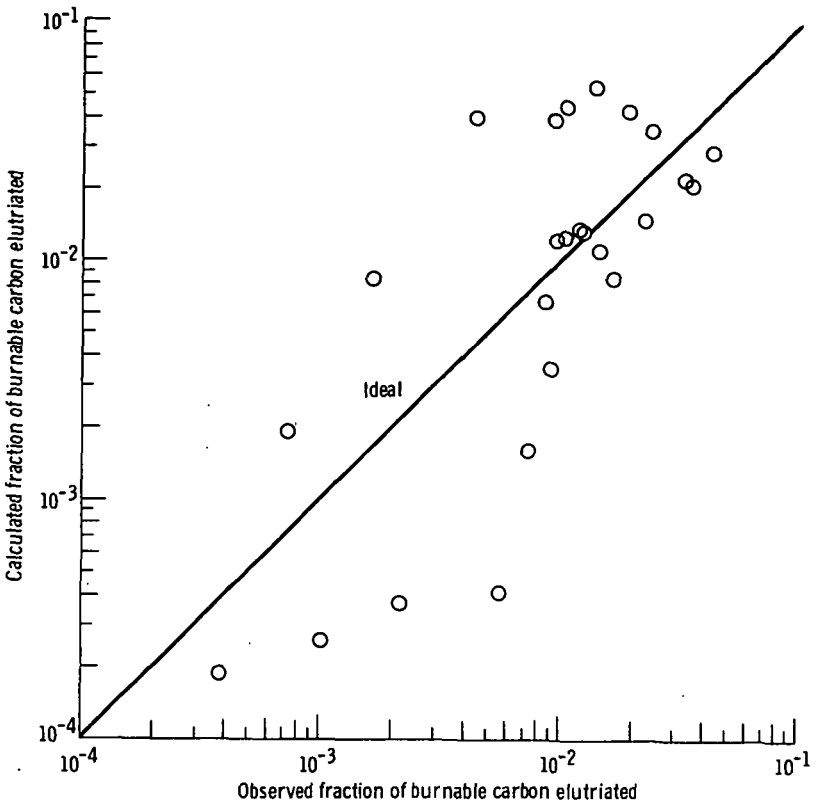

Figure 6. - Comparison of observed and calculated fraction of burnable carbon elutriated for cases 5 to 30 (theoretical elutriation (ref. 15) multiplied by BETA = 25).

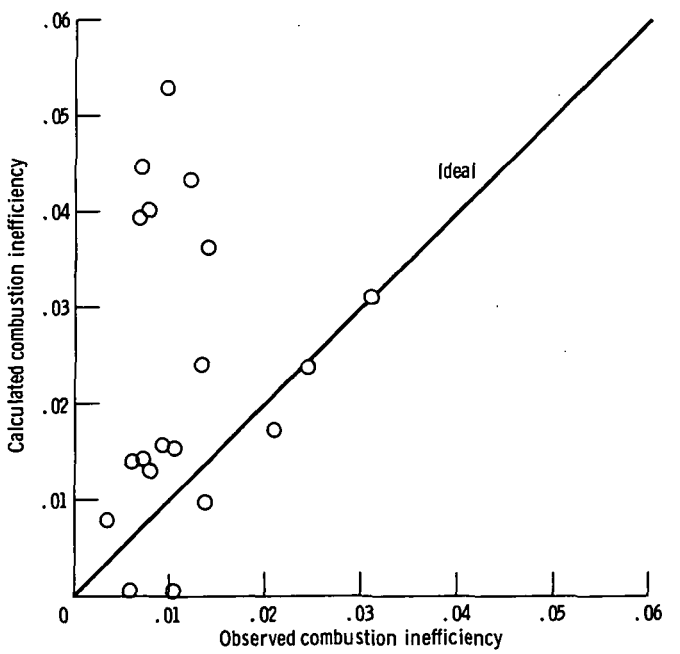

Figure 7. - Comparison of observed and calculated combustion inefficiencies for cases 5 to 30.

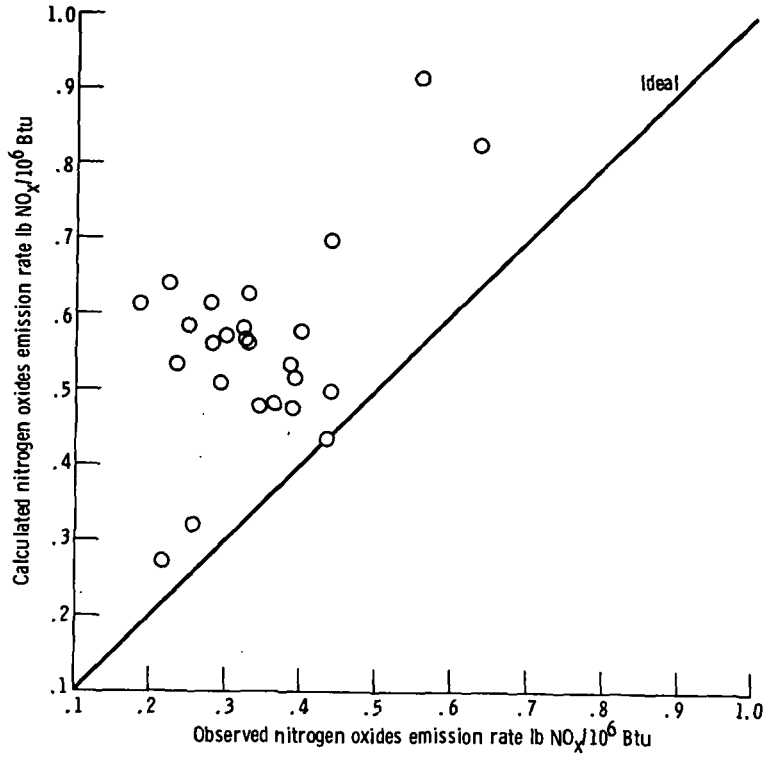

Figure 8. - Comparison of observed and calculated nitrogen oxides emission rate for cases 5 to 30.

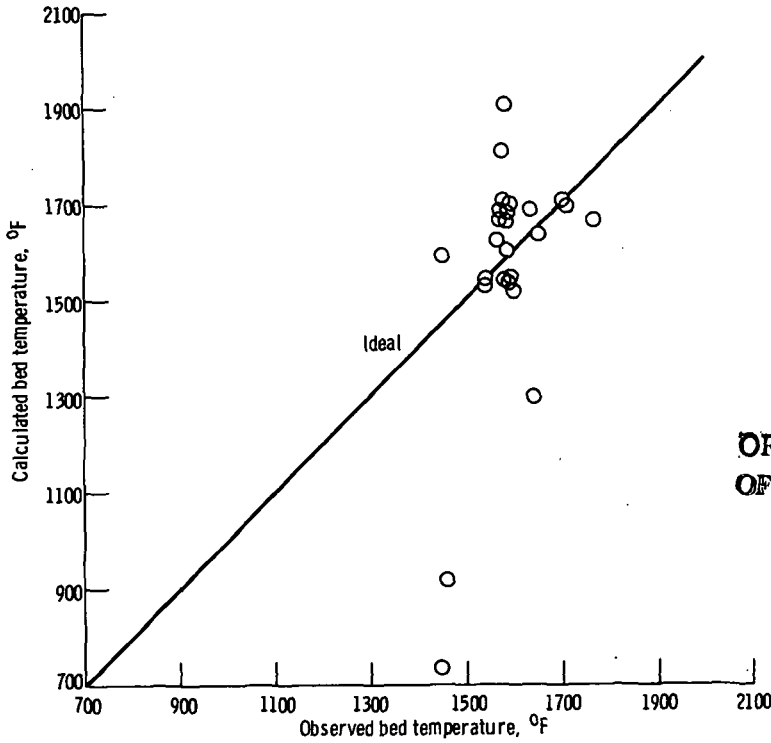

Figure 9. - Comparison of observed and calculated bed temperature at 14.7 inches above the distributor for cases 5 to 30.

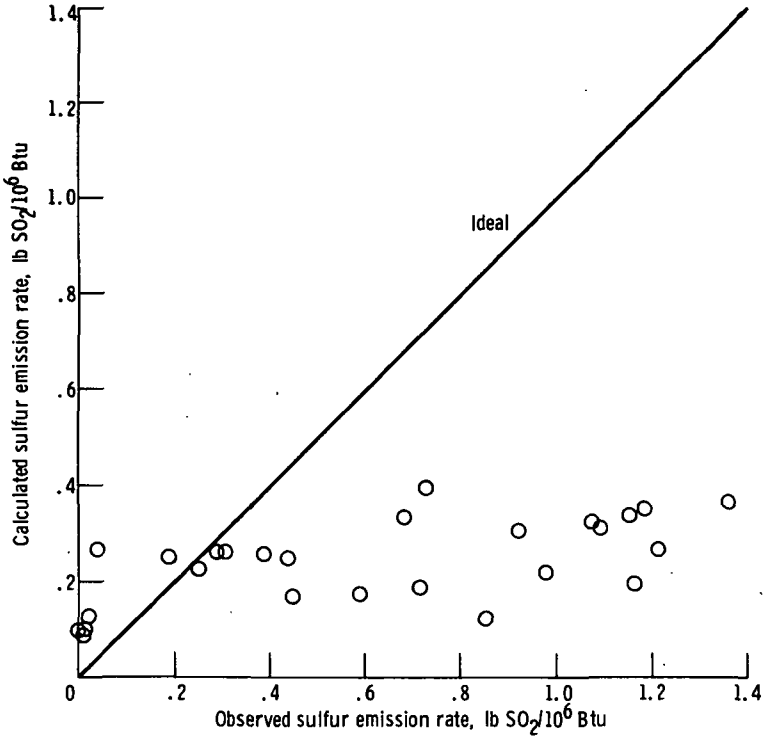

Figure 10. - Comparison of observed and calculated sulfur emission rate for cases 5 to 30.

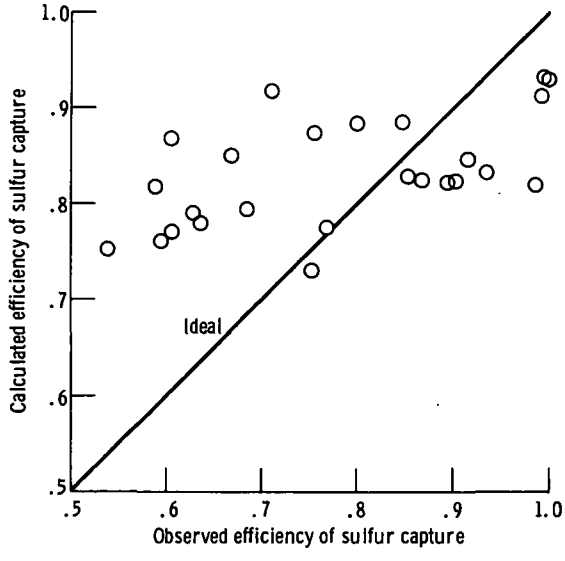

Figure 11. - Comparison of observed and calculated efficiency of sulfur capture for cases 5 to 30.

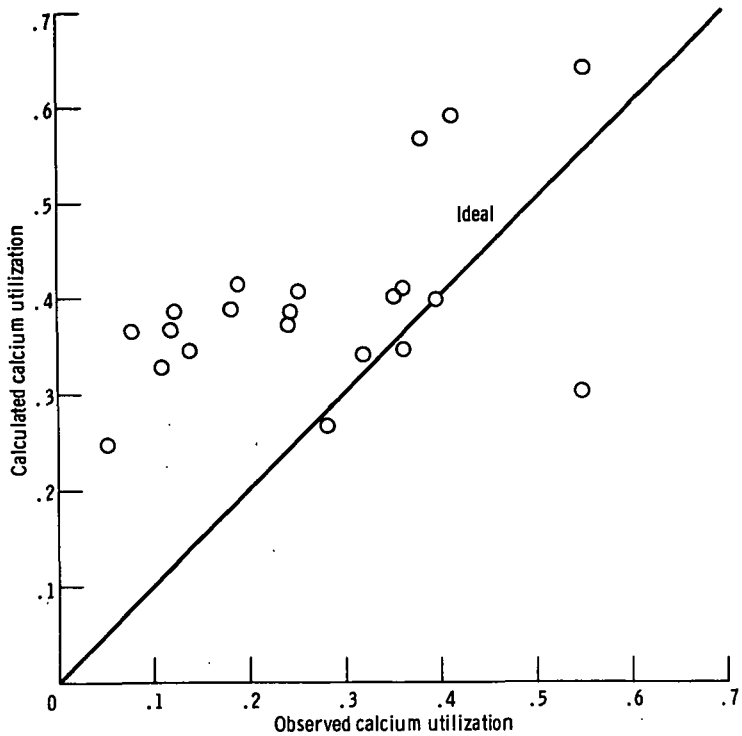

Figure 12. - Comparison of observed and calculated calcium utilization by limestone for cases 5 to 30.

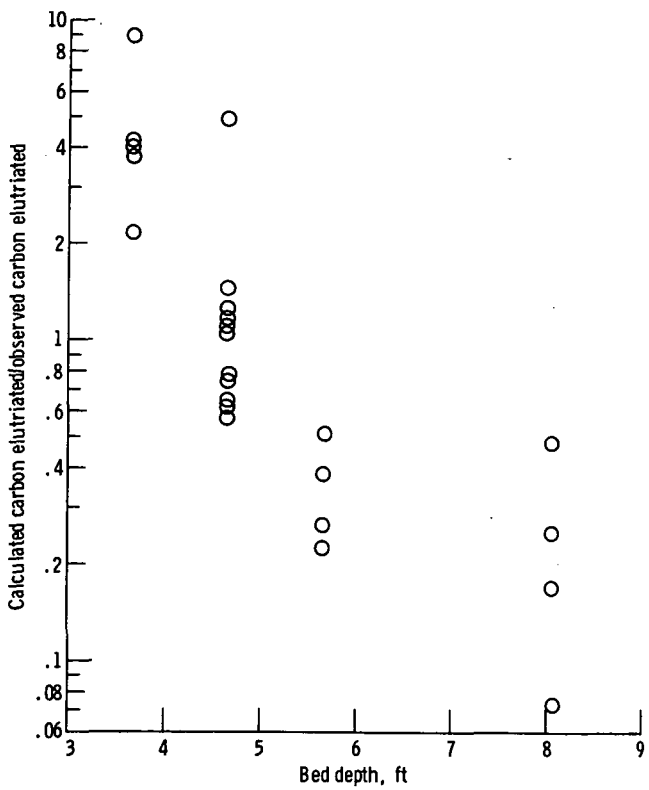

Figure 13. - Effect of bed depth on ratio of calculated to observed burnable carbon elutriated for cases 5 to 30 (theoretical elutriation (ref. 15) multiplied by BETA = 25).